THE GENERALIZED-α SCHEME AS A LINEAR MULTISTEP INTEGRATOR: TOWARD A GENERAL MECHATRONIC SIMULATOR

Olivier Brüls[1] and Martin Arnold[2]

[1]Department of Aerospace and Mechanical Engineering, University of Liège
Liège, B-4000, Belgium
Email: o.bruls@ulg.ac.be

[2]NWF III - Institute of Mathematics, Martin Luther University Halle-Wittenberg
Halle (Saale), D-06099, Germany
Email: martin.arnold@mathematik.uni-halle.de

Abstract

This paper presents a consistent formulation of the generalized-α time integration scheme for mechanical and mechatronic systems. The algorithm can deal with a non-constant mass matrix, controller dynamics, and kinematic constraints. The theoretical background relies on the analogy with linear multistep formulae, which leads to elegant results related with consistency, order conditions for constant and variable step-size methods, as well as global convergence. Those results are illustrated for a controlled spring-mass system, and the method is also applied for the simulation of a vehicle semi-active suspension.

INTRODUCTION

The generalized-α time integrator proposed by Chung and Hulbert [1] originates from the structural dynamics community, where it has been highly appreciated for its simple and efficient implementation as well as its ability to combine second-order accuracy with adjustable high-frequency numerical damping. Indeed, the equations of motion resulting from a finite element discretization are subject to spurious high-frequency modes which should ideally be filtered by the time integrator, without destroying the order of accuracy in the lower frequency range.

The properties of the constant step-size generalized-α integrator are well-known for linear mechanical structures represented by second-order differential equations. This paper investigates variable step-size algorithms for a broader class of dynamic systems, i.e. systems influenced by nonlinearities, kinematic constraints, and controller dynamics. In the literature, Erlicher *et al.* [2] have discussed the accuracy and stability of the generalized-α time integrator for nonlinear dynamic structures, Brüls and Golinval [3, 4, 5] have proposed a monolithic algorithm for coupled mechanical and control systems, Cardona and Géradin [6] have analysed the linear stability of the algorithm for mechanisms with kinematic constraints, and global convergence proofs have been published recently by Lunk and Simeon [7], Jay and Negrut [8], and Arnold and Brüls [9].

The present paper develops a unified theoretical framework based on the analogy between the generalized-α method and classical linear multistep formulae. Indeed, it is well-known that the generalized-α algorithm with fixed step-size is equivalent to a two step formula at velocity

level and to a three step formula at position level. In [9], this fact was used to extend the method to mechanical systems with a non-constant mass matrix. Let us mention that the resulting algorithm computes the acceleration variables with second-order accuracy, which is not the case for usual implementations of the method. In the context of mechatronic systems, the generalized-α method can be used to solve the first-order control state equation, as described in [3, 4, 5]. Here, the analogy with multistep formulae is further exploited for the design of a refined time integrator for mechatronic systems, which can deal with nonlinear acceleration feedbacks in a very natural way. This work also investigates the use of different integration formulae for the control state variables and the mechanical generalized coordinates.

On the one hand, we address the problem of variable step-size schemes. A variable step-size strategy tries to optimize the computational resources in order to satisfy a prescribed tolerance on the integration error at each time step, see, for instance, Géradin and Cardona [10]. Here, we show that an equivalence with linear multistep formulae still exists if the step-size is not constant. Using this equivalence, we also show that the classical second-order accuracy condition is not valid in this context. Actually, second-order accuracy requires a modification of the numerical parameters of the method at each time-step, depending on the step-size variations.

On the other hand, we demonstrate that the fixed step-size scheme exhibits several important convergence properties, i.e. that it is globally second-order accurate for a wide class of mechatronic problems. For unconstrained mechatronic systems, the importance of consistent initialization is highlighted and global convergence is demonstrated. A constrained mechanical system is represented by a set of differential-algebraic equations (DAEs) with index 3, see [11]. Lunk and Simeon [7] and Jay and Negrut [8] have proven convergence for regularized index-2 formulations, i.e. algorithms which make use of kinematic constraints at both position and velocity level. In [9], a convergence analysis was developed for an index-3 formulation, i.e. solely based on position level constraints. For the index-3 formulation, a simplified convergence analysis is described here, which is directly inspired by the theory of linear multistep methods for DAEs.

The theoretical results are illustrated for a controlled spring-mass system. Moreover, the method is applied for the simulation of a vehicle semi-active suspension.

THE GENERALIZED-α METHOD FOR MECHATRONIC SYSTEMS

In the present paper, the generalized-α method is applied to a class of mechatronic systems represented by the coupled equations [3]

$$\begin{aligned} \mathbf{M}(\mathbf{q})\ddot{\mathbf{q}} &= \mathbf{g}(\mathbf{q},\dot{\mathbf{q}},t) - \mathbf{\Phi}_{\mathbf{q}}^T\boldsymbol{\lambda} + \mathbf{L}\mathbf{y}, && (1)\\ \mathbf{0} &= \mathbf{\Phi}(\mathbf{q},t), && (2)\\ \dot{\mathbf{x}} &= \mathbf{f}(\mathbf{q},\dot{\mathbf{q}},\ddot{\mathbf{q}},\boldsymbol{\lambda},\mathbf{x},\mathbf{y},t), && (3)\\ \mathbf{y} &= \mathbf{h}(\mathbf{q},\dot{\mathbf{q}},\ddot{\mathbf{q}},\boldsymbol{\lambda},\mathbf{x},\mathbf{y},t), && (4) \end{aligned}$$

where $\mathbf{q}$ represents the mechanical generalized coordinates, $\boldsymbol{\lambda}$, the Lagrange multipliers, $\mathbf{x}$, the control state variables, and $\mathbf{y}$, the control output variables. Eqn. (1) describes the dynamics of the mechanical system, Eqn. (2), the kinematic constraints, Eqn. (3), the first-order control state dynamics and Eqn. (4) is the control output equation. In the first equation, $\mathbf{g}$ represents the external, internal and complementary inertia forces, and $\mathbf{\Phi}_{\mathbf{q}}$ is the constraint gradient. The mass matrix is not necessarily constant but it may depend on the generalized coordinates $\mathbf{q}$, which allows to cover the case of mechanical systems with large rotations.

The controller is influenced by input measurements from the mechanical system, which can be positions $\mathbf{q}$, velocities $\dot{\mathbf{q}}$, accelerations $\ddot{\mathbf{q}}$ or internal forces $\boldsymbol{\lambda}$, whereas the mechanical system is driven by control forces $\mathbf{L}\mathbf{y}$, where $\mathbf{L}$ is a constant boolean matrix. According to [3, 4], the coupled equations of motion can be formulated in a unified and modular environment: the

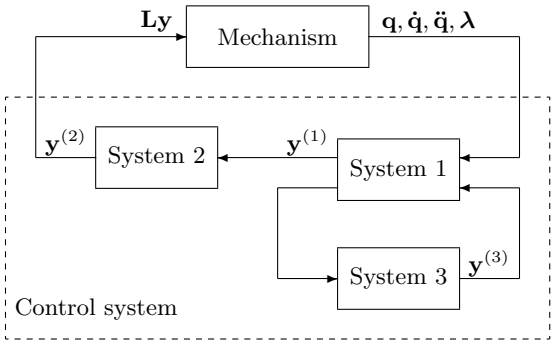

Figure 1: Block diagram model of a mechatronic system.

mechanical system is modeled using the finite element approach for flexible multibody systems presented in [10], whereas the control system is described using the block diagram language. Hence, in Fig. 1, one observes that the control system is decomposed into several interconnected blocks, and that the output variables of one block can be used as an input for other blocks. For this reason, the output Eqn. (4) is implicit in $\mathbf{y}$.

Description of the algorithm

Unlike in structural dynamics, the equations of motion (1)–(4) are generally nonlinear in the accelerations $\ddot{\mathbf{q}}$. For this reason, the classical weighted residual formulation of the generalized-α method is not applicable in the present context. Alternatively, we propose a time integration scheme where the dynamic equilibrium represented by Eqns. (1)–(4) is enforced exactly at each time step. Since the resulting formulation does not exploit a particular structure of those equations, it can be used even though the mass matrix is not constant and the control system includes nonlinear acceleration feedbacks.

Hence, the numerical variables $\mathbf{q}_{n+1}$, $\dot{\mathbf{q}}_{n+1}$, $\ddot{\mathbf{q}}_{n+1}$, $\boldsymbol{\lambda}_{n+1}$, $\mathbf{x}_{n+1}$, $\dot{\mathbf{x}}_{n+1}$ and $\mathbf{y}_{n+1}$ satisfy the coupled Eqns. (1)–(4) at time step $n+1$, whereas the vector $\mathbf{a}$ of acceleration-like variables is defined by the recurrence relation

$$(1-\alpha_m)\mathbf{a}_{n+1} + \alpha_m \mathbf{a}_n = (1-\alpha_f)\ddot{\mathbf{q}}_{n+1} + \alpha_f \ddot{\mathbf{q}}_n, \qquad \mathbf{a}_0 = \ddot{\mathbf{q}}_0. \tag{5}$$

We emphasize that $\mathbf{a}$ is an auxiliary variable, which is not equal to the true accelerations $\ddot{\mathbf{q}}$. Since $\mathbf{M}$ depends on $\mathbf{q}$, this equation cannot be restated as a weighted form of the mechanical dynamic equilibrium in Eqn. (1). The treatment of the state variables $\mathbf{x}$ and their derivative $\dot{\mathbf{x}}$ is similar to the treatment of the velocities $\dot{\mathbf{q}}$ and their derivative $\ddot{\mathbf{q}}$. Therefore, the auxiliary variable $\mathbf{w}$ is defined by

$$(1-\delta_m)\mathbf{w}_{n+1} + \delta_m \mathbf{w}_n = (1-\delta_f)\dot{\mathbf{x}}_{n+1} + \delta_f \dot{\mathbf{x}}_n, \qquad \mathbf{w}_0 = \dot{\mathbf{x}}_0. \tag{6}$$

The generalized-α scheme is obtained using $\mathbf{a}$ in the Newmark integration formulae

$$\mathbf{q}_{n+1} = \mathbf{q}_n + h\dot{\mathbf{q}}_n + h^2(0.5-\beta)\mathbf{a}_n + h^2\beta\mathbf{a}_{n+1}, \tag{7}$$

$$\dot{\mathbf{q}}_{n+1} = \dot{\mathbf{q}}_n + h(1-\gamma)\mathbf{a}_n + h\gamma\mathbf{a}_{n+1} \tag{8}$$

and $\mathbf{w}$ in the state integration formula

$$\mathbf{x}_{n+1} = \mathbf{x}_n + h(1-\theta)\mathbf{w}_n + h\theta\mathbf{w}_{n+1}. \tag{9}$$

Thus, seven algorithmic parameters α_m, α_f, β, γ, δ_m, δ_f and θ should thus be selected in order to obtain suitable accuracy and numerical stability properties.

Algorithm 1 solves Eqns. (5)-(9) together with the dynamic equilibrium at time t_{n+1}. The correction step involves the parameters

$$\beta' = \frac{1-\alpha_m}{h^2\beta(1-\alpha_f)}, \qquad \gamma' = \frac{\gamma}{h\beta}, \qquad \theta' = \frac{1-\delta_m}{h\theta(1-\delta_f)}$$

which satisfy the properties

$$\frac{\partial \ddot{\mathbf{q}}_{n+1}}{\partial \mathbf{q}_{n+1}} = \mathbf{I}\beta', \qquad \frac{\partial \dot{\mathbf{q}}_{n+1}}{\partial \mathbf{q}_{n+1}} = \mathbf{I}\gamma', \qquad \frac{\partial \dot{\mathbf{x}}_{n+1}}{\partial \mathbf{x}_{n+1}} = \mathbf{I}\theta',$$

and the iteration matrix is given by

$$\mathbf{S}_t = \left[\begin{array}{cc|cc} (\mathbf{M}\beta' - \mathbf{g}_{\dot{\mathbf{q}}}\gamma' + \mathbf{K}_t) & \mathbf{\Phi}_{\mathbf{q}}^T & \mathbf{0} & -\mathbf{L} \\ \mathbf{\Phi}_{\mathbf{q}} & \mathbf{0} & \mathbf{0} & \mathbf{0} \\ \hline (-\mathbf{f}_{\ddot{\mathbf{q}}}\beta' - \mathbf{f}_{\dot{\mathbf{q}}}\gamma' - \mathbf{f}_{\mathbf{q}}) & -\mathbf{f}_{\boldsymbol{\lambda}} & (\mathbf{I}\theta' - \mathbf{f}_{\mathbf{x}}) & -\mathbf{f}_{\mathbf{y}} \\ (-\mathbf{h}_{\ddot{\mathbf{q}}}\beta' - \mathbf{h}_{\dot{\mathbf{q}}}\gamma' - \mathbf{h}_{\mathbf{q}}) & -\mathbf{h}_{\boldsymbol{\lambda}} & -\mathbf{h}_{\mathbf{x}} & (\mathbf{I} - \mathbf{h}_{\mathbf{y}}) \end{array}\right]$$

with the tangent stiffness matrix $\mathbf{K}_t = \partial(\mathbf{M}\ddot{\mathbf{q}} - \mathbf{g} + \mathbf{\Phi}_{\mathbf{q}}^T\boldsymbol{\lambda})/\partial\mathbf{q}$. Compared to a classical algorithm based on a weighted residual formulation, Algorithm 1 involves similar computational resources. Indeed, it only requires two additional vectors $\mathbf{a}$ and $\mathbf{w}$, and the correction step, which is the most demanding part of the algorithm, is barely modified.

Since we are interested in variable step-size algorithms, the parameters γ, β and θ can be changed from one step to the next. When appropriate, the notations γ_n, β_n and θ_n will be used to denote their values in the argument list of the function `AlphaStep`.

Numerical parameters for fixed step-size algorithms

For a mechanical system represented by second-order ODEs, the generalized-α algorithm is second-order accurate provided that [1]

$$\gamma = 0.5 + \alpha_f - \alpha_m. \tag{10}$$

Likewise, for a control system represented by first-order ODEs, this condition becomes [12]

$$\theta = 0.5 + \delta_f - \delta_m. \tag{11}$$

These standard conditions are established for constant step-size algorithms, and an extension to variable step-size algorithms shall be developed later on.

For stiff problems, the solution should be computed accurately only in the low-frequency range, whereas the high-frequency solution should rather be damped out by the algorithm. The high-frequency numerical damping is represented by the spectral radius of the algorithm at infinity ρ_∞: an undamped scheme is characterized by $\rho_\infty = 1$, whereas $\rho_\infty = 0$ means asymptotic annihilation of the high-frequency response. For a given value of $\rho_\infty \in [0,1]$, Chung and Hulbert [1] have proposed optimal algorithmic parameters for second-order ODEs

$$\alpha_m = \frac{2\rho_\infty - 1}{\rho_\infty + 1}, \quad \alpha_f = \frac{\rho_\infty}{\rho_\infty + 1}, \quad \beta = 0.25\,(\gamma + 0.5)^2\,. \tag{12}$$

For first-order oscillatory ODEs, Jansen *et al.* [12] obtained

$$\delta_m = \frac{1}{2}\left(\frac{3\rho_\infty - 1}{\rho_\infty + 1}\right), \quad \delta_f = \frac{\rho_\infty}{\rho_\infty + 1}. \tag{13}$$

The algorithms defined by Eqns. (10) and (12) or by Eqns. (11) and (13) are stable when $h \to 0$ (zero-stability) and when $h \to \infty$ (stability). Since the optimal formulae are not equivalent for both sets of parameters, it is interesting to allow different integration schemes for the different subsystems (i.e. $\delta_f \neq \alpha_f$, $\delta_m \neq \alpha_m$ and $\theta \neq \gamma$).

Algorithm 1 $[\mathbf{q}_{n+1}, \dot{\mathbf{q}}_{n+1}, \ddot{\mathbf{q}}_{n+1}, \boldsymbol{\lambda}_{n+1}, \mathbf{x}_{n+1}, \dot{\mathbf{x}}_{n+1}, \mathbf{y}_{n+1}, \mathbf{a}, \mathbf{w}]$ = `AlphaStep`$(\mathbf{q}_n, \dot{\mathbf{q}}_n, \ddot{\mathbf{q}}_n, \mathbf{x}_n, \dot{\mathbf{x}}_n, \mathbf{a}, \mathbf{w}, \gamma, \beta, \theta, h)$

$\mathbf{q}_{n+1} := \mathbf{q}_n + h\dot{\mathbf{q}}_n + h^2(0.5 - \beta)\mathbf{a}$
$\dot{\mathbf{q}}_{n+1} := \dot{\mathbf{q}}_n + h(1 - \gamma)\mathbf{a}$
$\boldsymbol{\lambda}_{n+1} := \mathbf{0}$
$\mathbf{x}_{n+1} := \mathbf{x}_n + h(1 - \theta)\mathbf{w}$
$\mathbf{y}_{n+1} := \mathbf{0}$
$\mathbf{a} := 1/(1 - \alpha_m)(\alpha_f \ddot{\mathbf{q}}_n - \alpha_m \mathbf{a})$
$\mathbf{w} := 1/(1 - \delta_m)(\delta_f \dot{\mathbf{x}}_n - \delta_m \mathbf{w})$
$\mathbf{q}_{n+1} := \mathbf{q}_{n+1} + h^2\beta\mathbf{a}$
$\dot{\mathbf{q}}_{n+1} := \dot{\mathbf{q}}_{n+1} + h\gamma\mathbf{a}$
$\ddot{\mathbf{q}}_{n+1} := \mathbf{0}$
$\mathbf{x}_{n+1} := \mathbf{x}_{n+1} + h\theta\mathbf{w}$
$\dot{\mathbf{x}}_{n+1} := \mathbf{0}$
for $i = 1$ to i_{max} **do**
  Compute the residuals $\mathbf{r}^{\mathbf{q}}$ (Eqn. (1)), $\mathbf{r}^{\boldsymbol{\lambda}}$ (Eqn. (2)), $\mathbf{r}^{\mathbf{x}}$ (Eqn. (3)), $\mathbf{r}^{\mathbf{y}}$ (Eqn. (4))
  if $\sqrt{\|\mathbf{r}^{\mathbf{q}}\|^2 + \|\mathbf{r}^{\boldsymbol{\lambda}}\|^2 + \|\mathbf{r}^{\mathbf{x}}\|^2 + \|\mathbf{r}^{\mathbf{y}}\|^2} < tol$ **then**
    break
  end if
  $\begin{bmatrix} \Delta\mathbf{q} \\ \Delta\boldsymbol{\lambda} \\ \hline \Delta\mathbf{x} \\ \Delta\mathbf{y} \end{bmatrix} := -\mathbf{S}_t^{-1} \begin{bmatrix} \mathbf{r}^{\mathbf{q}} \\ \mathbf{r}^{\boldsymbol{\lambda}} \\ \hline \mathbf{r}^{\mathbf{x}} \\ \mathbf{r}^{\mathbf{y}} \end{bmatrix}$
  $\mathbf{q}_{n+1} := \mathbf{q}_{n+1} + \Delta\mathbf{q}$
  $\dot{\mathbf{q}}_{n+1} := \dot{\mathbf{q}}_{n+1} + \gamma'\Delta\mathbf{q}$
  $\ddot{\mathbf{q}}_{n+1} := \ddot{\mathbf{q}}_{n+1} + \beta'\Delta\mathbf{q}$
  $\boldsymbol{\lambda}_{n+1} := \boldsymbol{\lambda}_{n+1} + \Delta\boldsymbol{\lambda}$
  $\mathbf{x}_{n+1} := \mathbf{x}_{n+1} + \Delta\mathbf{x}$
  $\dot{\mathbf{x}}_{n+1} := \dot{\mathbf{x}}_{n+1} + \theta'\Delta\mathbf{x}$
  $\mathbf{y}_{n+1} := \mathbf{y}_{n+1} + \Delta\mathbf{y}$
end for
$\mathbf{a} := \mathbf{a} + (1 - \alpha_f)/(1 - \alpha_m)\ddot{\mathbf{q}}_{n+1}$
$\mathbf{w} := \mathbf{w} + (1 - \delta_f)/(1 - \delta_m)\dot{\mathbf{x}}_{n+1}$

Equivalent model

Assuming that the matrix

$$\begin{bmatrix} \mathbf{M} & -\mathbf{L} \\ -\mathbf{h}_{\ddot{\mathbf{q}}} & \mathbf{I} - \mathbf{h}_{\mathbf{y}} \end{bmatrix}$$

is non-singular, the implicit function theorem can be invoked to solve Eqns. (1) and (4) for $\ddot{\mathbf{q}}$ and $\mathbf{y}$. Hence, the dynamic equilibrium is equivalent to

$$\ddot{\mathbf{q}} = \mathbf{g}^*(\mathbf{q}, \dot{\mathbf{q}}, \boldsymbol{\lambda}, \mathbf{x}, t), \tag{14}$$
$$\mathbf{0} = \boldsymbol{\Phi}(\mathbf{q}, t), \tag{15}$$
$$\dot{\mathbf{x}} = \mathbf{f}^*(\mathbf{q}, \dot{\mathbf{q}}, \boldsymbol{\lambda}, \mathbf{x}, t), \tag{16}$$
$$\mathbf{y} = \mathbf{h}^*(\mathbf{q}, \dot{\mathbf{q}}, \boldsymbol{\lambda}, \mathbf{x}, t), \tag{17}$$

where the existence of the explicit functions $\mathbf{g}^*$ and $\mathbf{h}^*$ is guaranteed by the implicit function theorem. The function $\mathbf{f}^*$ is obtained after replacing $\ddot{\mathbf{q}}$ by the expression of $\mathbf{g}^*$ in the argument list of $\mathbf{f}$.

Since the dynamic equilibrium is enforced at every time step, the algorithm leads to the same solution when applied to the system (14)-(17). Moreover, the output variables are then fully decoupled, and it is sufficient to analyze the equivalent system (14)-(16). Hence, without any loss of generality, our theoretical investigations are performed for a model with the special form

$$\ddot{\mathbf{q}} = \mathbf{g}^*(\mathbf{q}, \dot{\mathbf{q}}, \boldsymbol{\lambda}, \mathbf{x}, t), \tag{18}$$
$$\mathbf{0} = \boldsymbol{\Phi}(\mathbf{q}, t), \tag{19}$$
$$\dot{\mathbf{x}} = \mathbf{f}(\mathbf{q}, \dot{\mathbf{q}}, \boldsymbol{\lambda}, \mathbf{x}, t). \tag{20}$$

In this case, the variables $\ddot{\mathbf{q}}$ and $\dot{\mathbf{x}}$ can be directly replaced by $\mathbf{g}^*$ and $\mathbf{f}$ in the integration formulae. Let us note that if the numerical solution is such that $\mathbf{q}_n$, $\dot{\mathbf{q}}_n$, $\boldsymbol{\lambda}_n$ and $\mathbf{x}_n$ are second-order accurate, the acceleration $\ddot{\mathbf{q}}_n$, which satisfies Eqn. (18), is also computed with second-order accuracy.

In addition, we assume that the system (18)-(20) has DAE index-3 [11], i.e. that the matrix

$$\boldsymbol{\Phi}_{\mathbf{q}} \mathbf{g}^*_{\boldsymbol{\lambda}}$$

is non-singular.

VARIABLE STEP-SIZE SCHEME

A variable step-size strategy tries to optimize the computational resources in order to reach a prescribed level of accuracy. Practically, the time step is selected in order to achieve a prescribed tolerance on the local integration error, see, for instance, Géradin and Cardona [10]. Assuming that the variations of the step-size are known, this section focuses on the order condition based on a multistep representation of the algorithm.

Multistep representation

Defining $h = t_{n+1} - t_n$ and s such that $t_n - t_{n-1} = h/s$, it is possible to eliminate $\mathbf{a}$ and $\mathbf{w}$ from the integration formulae at step n and $n+1$, leading to a two-step formulation

$$\begin{aligned}
\sum_{k=0}^{2} a_k \mathbf{q}_{n+k-1} + h \sum_{k=0}^{1} u_k \dot{\mathbf{q}}_{n+k-1} &= h^2 \sum_{k=0}^{2} b_k \mathbf{g}^*_{n+k-1}, && (21)\\
\sum_{k=0}^{2} a'_k \dot{\mathbf{q}}_{n+k-1} &= h \sum_{k=0}^{2} c_k \mathbf{g}^*_{n+k-1}, && (22)\\
\mathbf{0} &= \mathbf{\Phi}_{n+1}, && (23)\\
\sum_{k=0}^{2} d_k \mathbf{x}_{n+k-1} &= h \sum_{k=0}^{2} t_k \mathbf{f}_{n+k-1} && (24)
\end{aligned}$$

with the coefficients

$$\begin{array}{lll}
a_0 = -r\alpha_m, & a_1 = -1 + (1+r)\alpha_m, & a_2 = 1 - \alpha_m,\\
a'_0 = -r'\alpha_m, & a'_1 = -1 + (1+r')\alpha_m, & a'_2 = 1 - \alpha_m,\\
d_0 = -r''\delta_m, & d_1 = -1 + (1+r'')\delta_m, & d_2 = 1 - \delta_m,\\
u_0 = -(r/s)\alpha_m, & u_1 = -1 + \alpha_m, & \\
b_0 = (r/s^2)\alpha_f(1/2 - \beta_{n-1}), & b_1 = (r/s^2)(1-\alpha_f)(1/2-\beta_{n-1}) + \alpha_f\beta_n, & b_2 = (1-\alpha_f)\beta_n,\\
c_0 = (r'/s)\alpha_f(1-\gamma_{n-1}), & c_1 = (r'/s)(1-\alpha_f)(1-\gamma_{n-1}) + \alpha_f\gamma_n, & c_2 = (1-\alpha_f)\gamma_n,\\
t_0 = (r''/s)\delta_f(1-\theta_{n-1}), & t_1 = (r''/s)(1-\delta_f)(1-\theta_{n-1}) + \delta_f\theta_n, & t_2 = (1-\delta_f)\theta_n,
\end{array}$$

and

$$\begin{aligned}
r &= s^2(1-\alpha_m-2\beta_n)/(1-\alpha_m-2\beta_{n-1}),\\
r' &= s(1-\alpha_m-\gamma_n)/(1-\alpha_m-\gamma_{n-1}),\\
r'' &= s(1-\delta_m-\theta_n)/(1-\delta_m-\theta_{n-1}).
\end{aligned}$$

In the following, we seek for the values of β_n, γ_n and θ_n satisfying the order 2 condition.

Order condition

By definition, the method is *convergent of order two* if $\|\mathbf{q}(t_n) - \mathbf{q}_n\|$, $\|\dot{\mathbf{q}}(t_n) - \dot{\mathbf{q}}_n\|$ and $\|\mathbf{x}(t_n) - \mathbf{x}_n\|$ are $\mathcal{O}(h^2)$. In contrast, the *order two condition* means that the local error, i.e. the error after one time step, is $\mathcal{O}(h^3)$. It can be demonstrated [13] that this last condition is satisfied iff $\mathbf{l}^{\mathbf{q}}_n$, $\mathbf{l}^{\dot{\mathbf{q}}}_n$ and $\mathbf{l}^{\mathbf{x}}_n$ are $\mathcal{O}(h^3)$, where the defects $\mathbf{l}^{\mathbf{q}}_n$, $\mathbf{l}^{\dot{\mathbf{q}}}_n$ and $\mathbf{l}^{\mathbf{x}}_n$ are defined by introducing the exact solution $\mathbf{q}(t_n)$, $\dot{\mathbf{q}}(t_n)$, $\boldsymbol{\lambda}(t_n)$, $\mathbf{x}(t_n)$ into Eqns. (21), (22) and (24)

$$\begin{aligned}
\mathbf{l}^{\mathbf{q}}_n &= \sum_{k=0}^{2} a_k \mathbf{q}(t_{n+k-1}) + h \sum_{k=0}^{1} u_k \dot{\mathbf{q}}(t_{n+k-1}) - h^2 \sum_{k=0}^{2} b_k \mathbf{g}^*(t_{n+k-1}), && (25)\\
\mathbf{l}^{\dot{\mathbf{q}}}_n &= \sum_{k=0}^{2} a'_k \dot{\mathbf{q}}(t_{n+k-1}) - h \sum_{k=0}^{2} c_k \mathbf{g}^*(t_{n+k-1}), && (26)\\
\mathbf{l}^{\mathbf{x}}_n &= \sum_{k=0}^{2} d_k \mathbf{x}(t_{n+k-1}) - h \sum_{k=0}^{2} t_k \mathbf{f}(t_{n+k-1}), && (27)
\end{aligned}$$

with the notations $\mathbf{g}^*(t_n) = \mathbf{g}^*(\mathbf{q}(t_n), \dot{\mathbf{q}}(t_n), \boldsymbol{\lambda}(t_n), \mathbf{x}(t_n), t_n)$ and $\mathbf{f}(t_n) = \mathbf{f}(\mathbf{q}(t_n), \dot{\mathbf{q}}(t_n), \boldsymbol{\lambda}(t_n), \mathbf{x}(t_n), t_n)$.

In order to verify the order condition at the displacement level, Taylor series expansions

of the exact solution are introduced into Eqn. (25)

$$\begin{aligned}
\mathbf{q}(t_{n+1}) &= \mathbf{q}(t_n) + h\dot{\mathbf{q}}(t_n) + 0.5h^2\ddot{\mathbf{q}}(t_n) + \mathcal{O}(h^3),\\
\mathbf{q}(t_{n-1}) &= \mathbf{q}(t_n) - (h/s)\dot{\mathbf{q}}(t_n) + 0.5(h/s)^2\ddot{\mathbf{q}}(t_n) + \mathcal{O}(h^3),\\
\dot{\mathbf{q}}(t_{n-1}) &= \dot{\mathbf{q}}(t_n) - (h/s)\ddot{\mathbf{q}}(t_n) + \mathcal{O}(h^2),\\
\mathbf{g}^*(t_{n+1}) &= \ddot{\mathbf{q}}(t_n) + \mathcal{O}(h),\\
\mathbf{g}^*(t_{n-1}) &= \ddot{\mathbf{q}}(t_n) + \mathcal{O}(h).
\end{aligned}$$

After algebraic manipulations, we observe that the condition $\mathbf{l}_n^{\mathbf{q}} = \mathcal{O}(h^3)$ is automatically satisfied, which means that we can take $\beta_n = \beta$, as in the constant step-size algorithm.

At the velocity level, we use Eqn. (26) and the Taylor series expansions

$$\begin{aligned}
\dot{\mathbf{q}}(t_{n+1}) &= \dot{\mathbf{q}}(t_n) + h\ddot{\mathbf{q}}(t_n) + 0.5h^2\left(\frac{d^3\mathbf{q}}{dt^3}\right)(t_n) + \mathcal{O}(h^3),\\
\dot{\mathbf{q}}(t_{n-1}) &= \dot{\mathbf{q}}_n - (h/s)\ddot{\mathbf{q}}(t_n) + 0.5(h/s)^2\left(\frac{d^3\mathbf{q}}{dt^3}\right)(t_n) + \mathcal{O}(h^3),\\
\mathbf{g}^*(t_{n+1}) &= \ddot{\mathbf{q}}(t_n) + h\left(\frac{d^3\mathbf{q}}{dt^3}\right)(t_n) + \mathcal{O}(h^2),\\
\mathbf{g}^*(t_{n-1}) &= \ddot{\mathbf{q}}(t_n) - (h/s)\left(\frac{d^3\mathbf{q}}{dt^3}\right)(t_n) + \mathcal{O}(h^2).
\end{aligned}$$

The condition $\mathbf{l}_n^{\dot{\mathbf{q}}} = \mathcal{O}(h^3)$ is satisfied provided that

$$\frac{1-\alpha_m-\gamma_n}{1-\alpha_m-\gamma_{n-1}} = s\frac{(1-\alpha_f)\gamma_n - (1-\alpha_m)/2}{\alpha_f(1-\gamma_{n-1}) - \alpha_m/2}. \tag{28}$$

The value of γ_n can thus be deduced from the values of α_m, α_f, γ_{n-1} and s. In the case of fixed step-size ($s = 1$), if we impose $\gamma_n = \gamma_{n-1}$, this equation admits the solution $\gamma_n = 0.5+\alpha_f-\alpha_m$, which is the classical order condition already given in Eqn. (10). However, this solution is not unique since a degenerate solution $\gamma_n = 1-\alpha_m$ also exists. An interpretation of this additional solution will be given later on.

Finally, a condition similar to Eqn. (28) can be obtained for the first-order state variables, provided that γ_n, α_m and α_f are replaced by θ_n, δ_m and δ_f, respectively.

Sequence of γ_n coefficients

The value of γ_n should be updated at each time step according to Eqn. (28). A more practical equation is obtained using the change of variable $\gamma_n^* = 1-\alpha_m-\gamma_n$:

$$\gamma_n^* = \frac{s(1-\alpha_m)(0.5-\alpha_f)\gamma_{n-1}^*}{(\alpha_f + s(1-\alpha_f))\gamma_{n-1}^* - \alpha_m(0.5-\alpha_f)}. \tag{29}$$

If $s \neq -\alpha_f/(1-\alpha_f)$, this recursion can be written as

$$\gamma_n^* = \frac{a\gamma_{n-1}^*}{\gamma_{n-1}^* + b} \tag{30}$$

with $a = s(1-\alpha_m)(0.5-\alpha_f)/(\alpha_f + s(1-\alpha_f))$ and $b = -\alpha_m(0.5-\alpha_f)/(\alpha_f + s(1-\alpha_f))$.

It is important to check whether the values of γ_n (or γ_n^*) remain bounded during integration, at least in the case of a constant value of s. In this special case, a and b are also constant and the recursion (30) has two fixed points: $\gamma^* = 0$ and $\gamma^* = a - b$. If $s \neq |\alpha_m/(1-\alpha_m)|$, we have $|a/b| \neq 1$ and we can demonstrate that one of them is globally stable (or attractive). In

the case $|a/b| < 1$, let us show that γ_n^* converges to 0 if the initial value is different from $a - b$ (which implies that $\gamma_n^* \neq a - b, \forall n$). We consider the Lyapunov function

$$\mathcal{V}(\gamma^*) = \left(\frac{\gamma^*}{\gamma^* - a + b} \right)^2$$

which satisfies $\mathcal{V}(\gamma^*) > 0$, $\forall \gamma^* \neq 0$ and $\mathcal{V}(0) = 0$. Moreover, we have

$$\mathcal{V}(\gamma_n^*) - \mathcal{V}(\gamma_{n-1}^*) = \left(\frac{a^2}{b^2} - 1 \right) \left(\frac{\gamma_{n-1}^*}{\gamma_{n-1}^* - a + b} \right)^2 < 0$$

from which we conclude that γ_n^* converges asymptotically to 0. In the case $|a/b| > 1$, we can show that γ_n^* converges to $a - b$ using a similar argument and the Lyapunov function

$$\mathcal{V}(\gamma^*) = \left(\frac{\gamma^* - a + b}{\gamma^*} \right)^2.$$

Let us observe that the fixed point $\gamma^* = a - b$ corresponds to

$$\gamma = 1 - \alpha_m - (0.5 - \alpha_f) \frac{\alpha_m + s(1 - \alpha_m)}{\alpha_f + s(1 - \alpha_f)}$$

which gives the classical order condition $\gamma = 0.5 + \alpha_f - \alpha_m$ for $s = 1$. In contrast, the fixed point $\gamma^* = 0$ corresponds to the aforementioned degenerate solution $\gamma = 1 - \alpha_m$. For this value of γ, the two-step formulation is no more valid due to the singularity of the coefficient r'. Actually, the integration formula at velocity level can then be written as a one-step recursion

$$\dot{\mathbf{q}}_{n+1} - \dot{\mathbf{q}}_n = h\alpha_f \mathbf{g}_n + h(1 - \alpha_f)\mathbf{g}_{n+1},$$

which is only first order accurate unless $\alpha_f = 0.5$.

Hence, the condition $|a/b| > 1$, which makes the degenerate solution repulsive, seems favorable for the numerical behaviour of the algorithm. Using $a/b = -s(1 - \alpha_m)/\alpha_m$, this condition can be written as

$$s > s_{min} \quad \text{with} \quad s_{min} = \left| \frac{\alpha_m}{1 - \alpha_m} \right|.$$

Note that $s_{min} \leq 1$ for any practical algorithm since zero-stability requires $\alpha_m \leq 0.5$ (see below). For a constant step-size sequence ($s = 1$), the condition $|a/b| > 1$ is thus automatically fulfilled and the solution $\gamma = 0.5 + \alpha_f - \alpha_m$ is globally attractive.

CONSTANT STEP-SIZE SCHEME: CONVERGENCE ANALYSIS

In this section, additional convergence results are developed for constant step-size algorithms. In this case, the equivalent multistep formulation becomes simpler since we have

$$r = r' = r'' = 1 \quad \text{and} \quad a_i = a_i' \quad (i = 0, 1, 2). \tag{31}$$

Our objective is to prove that the classical order condition (10) implies global convergence. For this purpose, the multistep formulae in Eqns. (21), (22) and (24) are used to rewrite the defects

in Eqns. (25), (26) and (27) as

$$\mathbf{l}_n^{\mathbf{q}} = \sum_{k=0}^{2} a_k \mathbf{e}_{n+k-1}^{\mathbf{q}} + h \sum_{k=0}^{1} u_k \mathbf{e}_{n+k-1}^{\dot{\mathbf{q}}} - h^2 \sum_{k=0}^{2} b_k \mathbf{e}_{n+k-1}^{\mathbf{g}^*}, \tag{32}$$

$$\mathbf{l}_n^{\dot{\mathbf{q}}} = \sum_{k=0}^{2} a_k \mathbf{e}_{n+k-1}^{\dot{\mathbf{q}}} - h \sum_{k=0}^{2} c_k \mathbf{e}_{n+k-1}^{\mathbf{g}^*}, \tag{33}$$

$$\mathbf{l}_n^{\mathbf{x}} = \sum_{k=0}^{2} d_k \mathbf{e}_{n+k-1}^{\mathbf{x}} - h \sum_{k=0}^{2} t_k \mathbf{e}_{n+k-1}^{\mathbf{f}} \tag{34}$$

where $\mathbf{e}_n^{(\bullet)} = (\bullet)(t_n) - (\bullet)_n$ represent a global error after n steps. The stability of the error propagation process, which plays an important role in the convergence analysis, should be investigated in two extreme situations: $h \to 0$ and $h \to \infty$.

For $h \to 0$ (zero stability), the error propagation is stable during the integration process if the roots ζ_i of the polynomials

$$\sum_{k=0}^{2} a_k \zeta^k = 0, \quad \sum_{k=0}^{2} d_k \zeta^k = 0 \tag{35}$$

satisfy $|\zeta_i| \leq 1$, $i = 1, 2$. Since the first root is equal to 1, and the second are equal to $-\alpha_m/(1-\alpha_m)$ or $-\delta_m/(1-\delta_m)$, zero stability requires $\alpha_m \leq 0.5$ and $\delta_m \leq 0.5$. We note that all roots are necessarily simple.

For $h \to \infty$, the stability condition is developed separately for a control system and for a mechanical system. For a control system, the generalized-α method is stable if the roots ζ_i of the polynomial

$$\sum_{k=0}^{2} t_k \zeta^k = 0 \tag{36}$$

satisfy $|\zeta_i| \leq 1$, $i = 1, 2$. Since $\zeta_1 = -\delta_f/(1-\delta_f)$, and $\zeta_2 = -(1-\theta)/\theta$, this requires $\delta_f \leq 0.5$ and $\theta \geq 0.5$.

For a mechanical system, the stability analysis for $h \to \infty$ is based on the three step formulation of the integration scheme at position level

$$\sum_{k=0}^{3} a_k'' \mathbf{q}_{n+k-2} = h^2 \sum_{k=0}^{3} b_k'' \mathbf{g}_{n+k-2}^* \tag{37}$$

with the coefficients

$$\begin{aligned} &a_0'' = \alpha_m, \quad a_1'' = 1 - 3\alpha_m, \quad a_2'' = -2 + 3\alpha_m, \quad a_3'' = 1 - \alpha_m, \\ &b_0'' = \alpha_f(1/2 + \beta - \gamma), \quad b_1'' = (1-\alpha_f)(1/2 + \beta - \gamma) + \alpha_f(1/2 - 2\beta + \gamma), \\ &b_2'' = (1-\alpha_f)(1/2 - 2\beta + \gamma) + \alpha_f\beta, \quad b_3'' = (1-\alpha_f)\beta. \end{aligned} \tag{38}$$

The algorithm is stable if the roots ζ_i of the polynomials

$$\sum_{k=0}^{3} b_k'' \zeta^k = 0 \tag{39}$$

satisfy $|\zeta_i| \leq 1$, $i = 1, 2, 3$. Using the order two condition in Eqn. (10), this leads to the requirements $\alpha_m \leq \alpha_f \leq 0.5$ and $\beta \geq 0.25 + 0.5(\alpha_f - \alpha_m)$.

In the following, the convergence analysis is first realized for unconstrained systems represented by ODEs, and then for constrained systems represented by DAEs.

Unconstrained case

Theorem: a generalized-α algorithm which satisfies the zero stability and the order two conditions is convergent of order two for the system

$$\begin{aligned} \ddot{\mathbf{q}} &= \mathbf{g}^*(\mathbf{q}, \dot{\mathbf{q}}, \mathbf{x}, t), \\ \dot{\mathbf{x}} &= \mathbf{f}(\mathbf{q}, \dot{\mathbf{q}}, \mathbf{x}, t). \end{aligned}$$

Proof: The demonstration is composed of three parts. The first two parts focus on the special case of a state space system $\dot{\mathbf{x}} = \mathbf{f}(\mathbf{x}, t)$, and the extension to mechatronic systems is presented in the third part.

Global error estimation.

In order to estimate the error after several time steps, we proceed in a recursive way, i.e. we express the error at time $n+1$ in terms of the local error and the error at the past steps. For a smooth function $\mathbf{f}$, we can use

$$\mathbf{e}_n^{\mathbf{f}} = \mathcal{O}(1)\|\mathbf{e}_n^{\mathbf{x}}\|.$$

Introducing this expression into Eqn. (34), and using the order condition, the desired recursion formula is obtained

$$\mathbf{e}_{n+1}^{\mathbf{x}} = -\frac{d_0}{d_2}\mathbf{e}_{n-1}^{\mathbf{x}} - \frac{d_1}{d_2}\mathbf{e}_n^{\mathbf{x}} + \mathcal{O}(h)\sum_{k=0}^{2}\|\mathbf{e}_{n+k-1}^{\mathbf{x}}\| + \frac{1}{d_2}\mathbf{l}_n^{\mathbf{x}}. \tag{40}$$

Defining

$$\mathbf{E}_n = \begin{pmatrix} \mathbf{e}_n^{\mathbf{x}} \\ \mathbf{e}_{n-1}^{x} \end{pmatrix}, \quad \mathbf{L}_n = \begin{pmatrix} \mathbf{l}_n^{\mathbf{x}}/d_2 \\ \mathbf{0} \end{pmatrix}, \quad \mathbf{A} = \begin{pmatrix} -\frac{d_1}{d_2}\mathbf{I} & -\frac{d_0}{d_2}\mathbf{I} \\ \mathbf{I} & \mathbf{0} \end{pmatrix},$$

Eqn. (40) becomes a one step recursion [13, section III.4]

$$\mathbf{E}_{n+1} = \mathbf{A}\mathbf{E}_n + \mathcal{O}(h)\left(\|\mathbf{E}_n\| + \|\mathbf{E}_{n+1}\|\right) + \mathbf{L}_n.$$

Using the zero stability condition, the eigenvalues ζ_i of the propagation matrix $\mathbf{A}$ are such that $|\zeta_i| \leq 1$. Moreover, there is no multiple eigenvalue and we are thus able to fix a constant C such that

$$\|\mathbf{E}_{n+1}\| \leq (1 + hC)\left(\|\mathbf{E}_n\| + \|\mathbf{L}_n\|\right).$$

Restating the order condition as $\|\mathbf{L}_n\| \leq Mh^3$, and following the arguments described by Hairer *et al.* [13] (Lady Windermere's fan), the global estimate after n steps is obtained

$$\|\mathbf{E}_n\| \leq \|\mathbf{E}_0\|e^{nhC} + \frac{Mh^2}{C}(e^{nhC} - 1)$$

which demonstrates that the global error is $\mathcal{O}(h^2)$ if the initial values satisfy $\|\mathbf{E}_0\| = \mathcal{O}(h^2)$.

Initial value condition.

The initial values should satisfy $\|\mathbf{E}_0\| = \mathcal{O}(h^2)$, which means that we need $\|\mathbf{x}(t_0) - \mathbf{x}_0\| = \mathcal{O}(h^2)$ and $\|\mathbf{x}(t_{-1}) - \mathbf{x}_{-1}\| = \mathcal{O}(h^2)$. The former condition is satisfied since $\mathbf{x}_0 = \mathbf{x}(t_0)$, but the second requires a more detailed analysis. For this purpose, we observe that the virtual quantity $\mathbf{x}_{-1}$ satisfies the integration formula

$$\mathbf{x}_0 = \mathbf{x}_{-1} + h(1-\theta)\mathbf{w}_{-1} + h\theta\mathbf{w}_0$$

where $\mathbf{w}_{-1}$ is defined by

$$(1-\delta_m)\mathbf{w}_0 + \delta_m\mathbf{w}_{-1} = (1-\delta_f)\mathbf{f}_0 + \delta_f\mathbf{f}_{-1}.$$

Using the condition $\mathbf{w}_0 = \mathbf{f}_0$, as well as $\mathbf{f}_{-1} = \mathbf{f}_0 + \mathcal{O}(\|\mathbf{x}_{-1} - \mathbf{x}_0\|)$, we get

$$\mathbf{w}_{-1} = \mathbf{f}_0 + \mathcal{O}(\|\mathbf{x}_{-1} - \mathbf{x}_0\|)$$

so that

$$\mathbf{x}_{-1} = \mathbf{x}_0 - h\mathbf{f}_0 + h\mathcal{O}(\|\mathbf{x}_{-1} - \mathbf{x}_0\|).$$

From this result, we have $\|\mathbf{x}_{-1} - \mathbf{x}_0\| = \mathcal{O}(h)$, and the final conclusion follows since $\mathbf{x}(t_{-1}) = \mathbf{x}_0 - h\mathbf{f}_0 + \mathcal{O}(h^2)$.

Mechatronic systems.

The previous analysis can be reproduced for mechatronic systems if we redefine

$$\mathbf{E}_n = \begin{pmatrix} \mathbf{e}_n^{\mathbf{q}} \\ \mathbf{e}_{n-1}^{\mathbf{q}} \\ \mathbf{e}_n^{\dot{\mathbf{q}}} \\ \mathbf{e}_{n-1}^{\dot{\mathbf{q}}} \\ \mathbf{e}_n^{\mathbf{x}} \\ \mathbf{e}_{n-1}^{\mathbf{x}} \end{pmatrix}, \quad \mathbf{L}_n = \begin{pmatrix} \mathbf{l}_n^{\mathbf{q}}/a_2 \\ \mathbf{0} \\ \mathbf{l}_n^{\dot{\mathbf{q}}}/a_2 \\ \mathbf{0} \\ \mathbf{l}_n^{\mathbf{x}}/d_2 \\ \mathbf{0} \end{pmatrix}, \quad \mathbf{A} = \left(\begin{array}{cc|cc|cc} -\frac{a_1}{a_2}\mathbf{I} & -\frac{a_0}{a_2}\mathbf{I} & & & & \\ \mathbf{I} & \mathbf{0} & & & & \\ \hline & & -\frac{a_1}{a_2}\mathbf{I} & -\frac{a_0}{a_2}\mathbf{I} & & \\ & & \mathbf{I} & \mathbf{0} & & \\ \hline & & & & -\frac{d_1}{d_2}\mathbf{I} & -\frac{d_0}{d_2}\mathbf{I} \\ & & & & \mathbf{I} & \mathbf{0} \end{array}\right)$$

where the blanks in matrix $\mathbf{A}$ represent null blocks, which indicates a decoupled error propagation of the various components. If the two zero-stability conditions are fulfilled, the eigenvalues ζ_i of the propagation matrix $\mathbf{A}$ are such that $|\zeta_i| \leq 1$. As previously, we conclude that the global error is $\mathcal{O}(h^2)$ since the initial values satisfy $\|\mathbf{E}_0\| = \mathcal{O}(h^2)$.

Constrained case

To simplify the presentation, let us consider the system

$$\begin{aligned} \ddot{\mathbf{q}} &= \mathbf{g}^*(\mathbf{q}, \dot{\mathbf{q}}, \boldsymbol{\lambda}, t), \\ \mathbf{0} &= \boldsymbol{\Phi}(\mathbf{q}, t). \end{aligned}$$

The extension to general mechatronic systems does not represent a major difficulty.

This section presents the sketch of a global convergence analysis and we refer to [14] for technical details. As in the unconstrained case, the analysis of the error propagation is based on the defect Eqns. (32) and (33). The major difficulty comes from the lack of *a priori* information on the local error in the multipliers. We thus define the projectors

$$\mathbf{Q}_n = \left(\mathbf{g}_{\boldsymbol{\lambda}}^*(\boldsymbol{\Phi}_{\mathbf{q}}\mathbf{g}_{\boldsymbol{\lambda}}^*)^{-1}\boldsymbol{\Phi}_{\mathbf{q}}\right)(t_n), \qquad \mathbf{P}_n = \mathbf{I} - \mathbf{Q}_n,$$

with the properties

$$\mathbf{Q}_n\mathbf{g}_{\boldsymbol{\lambda}}^*(t_n) = \mathbf{g}_{\boldsymbol{\lambda}}^*(t_n), \quad \mathbf{P}_n\mathbf{g}_{\boldsymbol{\lambda}}^*(t_n) = \mathbf{0}.$$

$\mathbf{P}_n$ represents a projection onto the tangent space, whereas $\mathbf{Q}_n$ represents a projection in the oblique direction (see Fig. 2). For a purely mechanical system with $\mathbf{M} = \mathbf{I}$, we have $\mathbf{g}_{\boldsymbol{\lambda}}^* = -\boldsymbol{\Phi}_{\mathbf{q}}^T$ and the two projections are orthogonal.

Let us define the vectors

$$\mathbf{E}_n^{\mathbf{P}\mathbf{q}} = \begin{pmatrix} \mathbf{P}_n\mathbf{e}_n^{\mathbf{q}} \\ \mathbf{P}_{n-1}\mathbf{e}_{n-1}^{\mathbf{q}} \end{pmatrix}, \quad \mathbf{E}_n^{\mathbf{P}\dot{\mathbf{q}}} = \begin{pmatrix} \mathbf{P}_n\mathbf{e}_n^{\dot{\mathbf{q}}} \\ \mathbf{P}_{n-1}\mathbf{e}_{n-1}^{\dot{\mathbf{q}}} \end{pmatrix}, \quad \mathbf{E}_n^{\mathbf{Q}\dot{\mathbf{q}}} = \begin{pmatrix} \mathbf{Q}_n\mathbf{e}_n^{\dot{\mathbf{q}}} \\ \mathbf{Q}_{n-1}\mathbf{e}_{n-1}^{\dot{\mathbf{q}}} \end{pmatrix}, \quad \mathbf{E}_n^{h\boldsymbol{\lambda}} = \begin{pmatrix} \mathbf{e}_n^{h\boldsymbol{\lambda}} \\ \mathbf{e}_{n-1}^{h\boldsymbol{\lambda}} \\ \mathbf{e}_{n-2}^{h\boldsymbol{\lambda}} \end{pmatrix}.$$

If the zero stability condition is enforced strictly ($\alpha_m < 0.5$), the algorithm is strictly stable (e.g. Eqn. (12) with $\rho_\infty < 1$), and the second-order condition is verified, it is possible to demonstrate

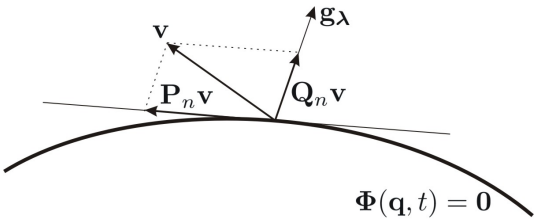

Figure 2: Projections of a vector $\mathbf{v}$ in the $\mathbf{q}$-space (t is frozen).

that the error propagation satisfies:

$$\begin{pmatrix} \|\mathbf{E}_{n+1}^{\mathbf{Pq}}\| \\ \|\mathbf{E}_{n+1}^{\mathbf{P\dot{q}}}\| \\ \|\mathbf{E}_{n+1}^{\mathbf{Q\dot{q}}}\| \\ \|\mathbf{E}_{n+1}^{h\boldsymbol{\lambda}}\| \end{pmatrix} \leq \begin{pmatrix} \mathcal{O}(h^3) \\ \mathcal{O}(h^3) \\ \mathcal{O}(h^2) \\ \mathcal{O}(h^2) \end{pmatrix} + \left(\begin{array}{cc|cc} 1+\mathcal{O}(h) & \mathcal{O}(h) & \mathcal{O}(h^2) & \mathcal{O}(h^2) \\ \mathcal{O}(h) & 1+\mathcal{O}(h) & \mathcal{O}(h) & \mathcal{O}(h) \\ \hline \mathcal{O}(1) & \mathcal{O}(h) & \rho_1+\mathcal{O}(h) & \mathcal{O}(1) \\ \mathcal{O}(1) & \mathcal{O}(h) & \mathcal{O}(h) & \rho_2+\mathcal{O}(h) \end{array}\right) \begin{pmatrix} \|\mathbf{E}_{n}^{\mathbf{Pq}}\| \\ \|\mathbf{E}_{n}^{\mathbf{P\dot{q}}}\| \\ \|\mathbf{E}_{n}^{\mathbf{Q\dot{q}}}\| \\ \|\mathbf{E}_{n}^{h\boldsymbol{\lambda}}\| \end{pmatrix}$$

with $\rho_1 < 1$ and $\rho_2 < 1$. We deduce, as in [14], that the global errors after n steps satisfy

$$\begin{pmatrix} \|\mathbf{E}_{n}^{\mathbf{Pq}}\| \\ \|\mathbf{E}_{n}^{\mathbf{P\dot{q}}}\| \\ \|\mathbf{E}_{n}^{\mathbf{Q\dot{q}}}\| \\ \|\mathbf{E}_{n}^{h\boldsymbol{\lambda}}\| \end{pmatrix} = \mathcal{O}(1)\left(\|\mathbf{E}_{0}^{\mathbf{Pq}}\| + \|\mathbf{E}_{0}^{\mathbf{P\dot{q}}}\| + \|\mathbf{E}_{0}^{\mathbf{Q\dot{q}}}\| + \|\mathbf{E}_{0}^{h\boldsymbol{\lambda}}\|\right) + \mathcal{O}(h^2).$$

The global error for the multipliers $\mathbf{e}_n^{\boldsymbol{\lambda}}$ is thus $\mathcal{O}(h)$, whereas the global errors for $\mathbf{q}$ and $\dot{\mathbf{q}}$ are $\mathcal{O}(h^2)$. However, this result appears to be conservative: in a recent work, $\mathcal{O}(h^2)$ convergence could also be demonstrated for the multipliers [9].

APPLICATIONS

Controlled spring-mass system

In the first example, the active damping of a one degree-of-freedom spring-mass system is analyzed. The mechanical equation of motion is

$$m\ddot{q} + kq = g^a$$

where m is the mass, k is the stiffness of the spring, and g^a denotes the force exerted by the actuator. The desired actuator force g^d is determined by a feedback law based on acceleration measurements

$$\begin{aligned} \dot{x} &= -\sigma x - b\ddot{q}, \\ g^d &= x. \end{aligned}$$

Let us note that if $\sigma \to 0$, the desired force g^d becomes equal to a direct velocity feedback $-b\dot{q}$, which has a stabilizing effect if $b > 0$. In practice, a positive value σ is selected in order to filter possible low-frequency disturbances in the acceleration measurements, which would be otherwise amplified by the controller. The actuator is characterized by a saturation at the value g^{max}. The relation between the command g^d and the actual force is thus modelled according to

$$g^a = g^{max}\tanh(g^d/g^{max}).$$

If the vector of output variables $\mathbf{y}^T = [g^d,\ g^a]$ is defined, the model of this mechatronic system has the structure of Eqns.(1)-(4), and can thus be implemented using our formalism. In the

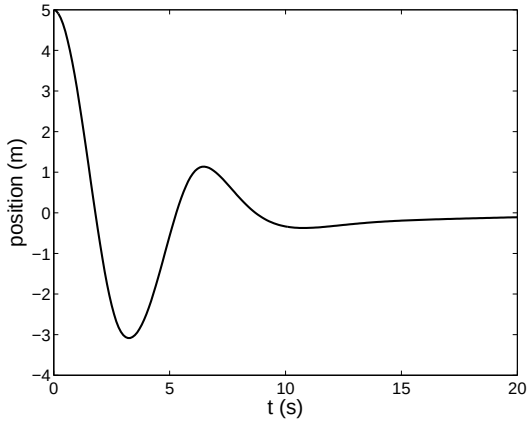

Figure 3: Position of the mass.

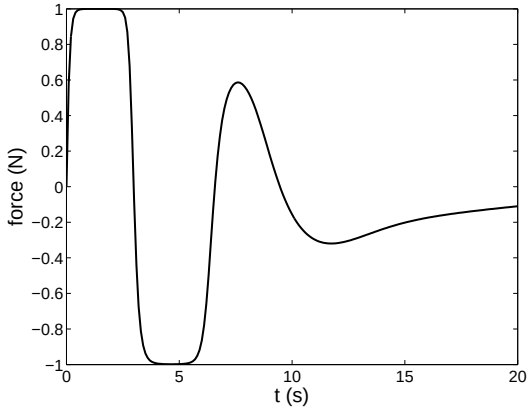

Figure 4: Actuator force.

previous theoretical investigations, we also used the equivalent form (18)-(20), which becomes, in this particular case,

$$\begin{aligned} \ddot{q} &= -(k/m)q + (g^{max}/m)\tanh(x/g^{max}), \\ \dot{x} &= -\sigma x + (bk/m)q - (bg^{max}/m)\tanh(x/g^{max}). \end{aligned}$$

The system is initially released from a position $q(0) = q_0$ with $\dot{q}(0) = 0$ and $x(0) = 0$. At acceleration level, consistent initial conditions are thus given by

$$\begin{aligned} \ddot{q}_0 &= -(k/m)q_0, \\ \dot{x}_0 &= (bk/m)q_0. \end{aligned}$$

For the numerical simulations, the values $m = 1$ kg, $k = 1$ N/m, $\sigma = 0.1$ s^{-1}, $b = 1.4$ Ns/m, $g^{max} = 1$ N, and $q_0 = 5$ m have been considered. The nominal step-size is fixed to $h = 0.1$ s, and the algorithmic parameters are selected according to Eqns. (10)-(13) with $\rho_\infty = 0.8$.

Simulation results are given in Figs. 3 and 4. During the first ten seconds, the nonlinear effects caused by the saturation of the actuator force have a significant influence on the dynamic behaviour. During the last ten seconds, the energy in the system is reduced and nonlinear phenomena become less important.

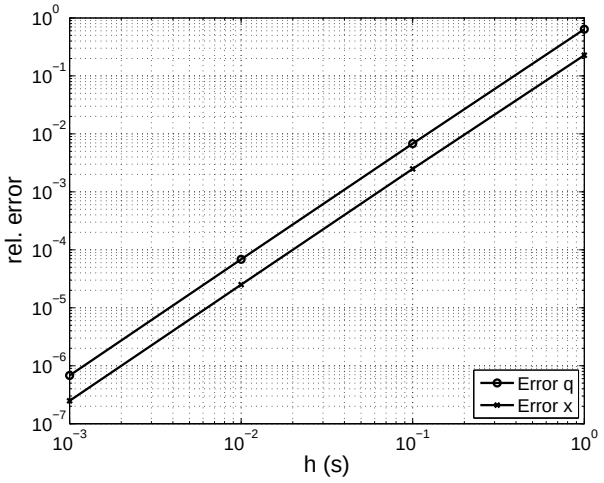

Figure 5: Convergence of the simulation results (fixed step-size).

A convergence analysis of the fixed step-size algorithm is shown in Fig. 5. The relative errors in the values of q and x at time $t = 5$ s are plotted with respect to the step-size value and, as predicted by the theory, we observe that the errors decrease as $\mathcal{O}(h^2)$. Let us mention that the reference solution was obtained using a very small step-size $h =$ 1.e-4 s.

A numerical experiment is also realized to illustrate the order condition developed for variable step-size schemes. The simulation has been realized using an alternated sequence of step-sizes: the time interval is decomposed in a number of macro-steps of size H, and each macro-step is itself decomposed into two steps of size $0.3H$ and $0.7H$. In Fig. 6, a convergence analysis is presented for decreasing values of H. As before, the reference solution was computed using a fixed step-size $h =$ 1.e-4 s. The algorithm with fixed values $\gamma = 0.5 + \alpha_f - \alpha_m$ and $\theta = 0.5 + \delta_f - \delta_m$ is compared to the algorithm with updated values of γ and θ (see Eqn. (29)). The results clearly demonstrate that the update of γ and θ is required to observe second-order convergence.

Semi-active suspension

The generalized-α algorithm described in this paper is applied to the simulation of a car equipped with a semi-active suspension. This benchmark has been developed in the framework of the Belgian Inter-University Attraction Pole on Advanced Mechatronic Systems (AMS-IAP5/06).

The semi-active actuator, which is controlled by an electrical valve, is mounted in parallel with a passive spring. The control law exploits information from accelerometers placed at the four corners of the chassis (Fig. 7), and from linear displacement sensors measuring the extension of the four shock-absorbers. The model of the mechatronic system is composed of a mechanical model, a model of the actuators, and a model of the controller. A detailed description of the actuators and of the controller is presented by Lauwerys et al. [15].

The rigid-body model of the car, which is illustrated in Fig. 8, includes the car-body, the chassis, rear and front multi-link suspension mechanisms with passive springs, the slider crank direction mechanism for the front wheels and the tyre model. The 3D mechanical model, which has been developed according to the formalism presented by Géradin and Cardona [10], involves a total of 600 degrees-of-freedom, numerous revolute and prismatic joints, several closed-loops and four wheel-ground contact models. It could be later extended to include the stiffness of the suspension bushings, the flexibility of the chassis, and a longitudinal model for the wheels.

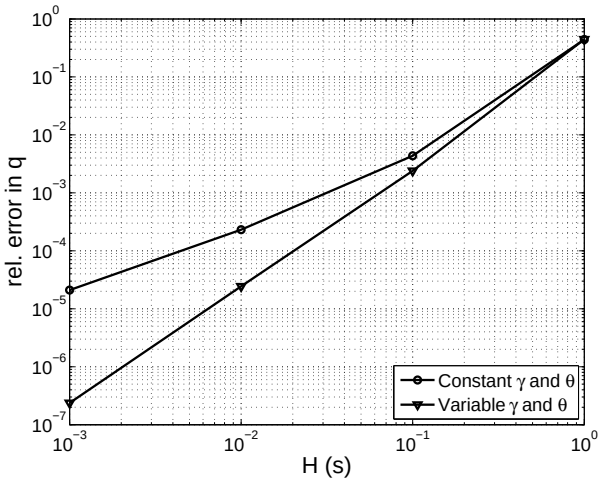

Figure 6: Convergence of the simulation results (variable step-size).

Figure 7: Audi A6 - Corner accelerometers.

Figure 9 illustrates the principle of a semi-active actuator. The actuator model is described in nonlinear state-space format

$$\begin{aligned} \dot{\mathbf{x}}^{(damp)} &= \mathbf{f}^{(damp)}(\mathbf{u}^{(damp)}, \mathbf{x}^{(damp)}), \\ \mathbf{y}^{(damp)} &= \mathbf{h}^{(damp)}(\mathbf{u}^{(damp)}, \mathbf{x}^{(damp)}) \end{aligned}$$

with the inputs, states and output

$$\begin{aligned} \mathbf{u}^{(damp)} &= [l \quad dl/dt \quad i]^T, \\ \mathbf{x}^{(damp)} &= [p^{reb} \quad p^{comp}]^T, \\ \mathbf{y}^{(damp)} &= [g^a]. \end{aligned}$$

l is the actuator extension, i, the electrical current in the valve, p^{reb} and p^{comp}, the pressures in the rebound and compression chambers, and g^a, the force exerted by the damper. The functions $\mathbf{f}^{(damp)}$ and $\mathbf{h}^{(damp)}$ are given by the manufacturer of the shock-absorber as C-functions.

The control law, available as a block diagram model, consists of three stages (Fig. 10): a feedback linearization (inverse actuator model), a transformation of the actuator forces and of the acceleration measurements into modal space (heave, roll, and pitch), and a linear integral

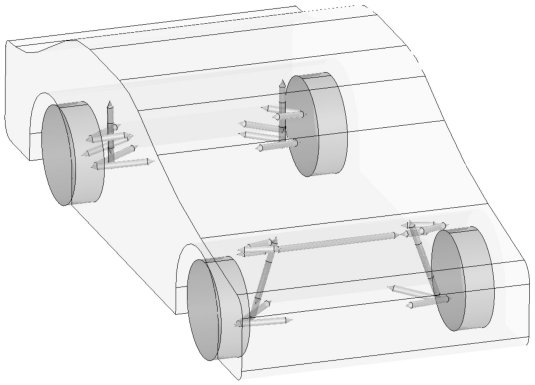

Figure 8: Mechanical model of the car.

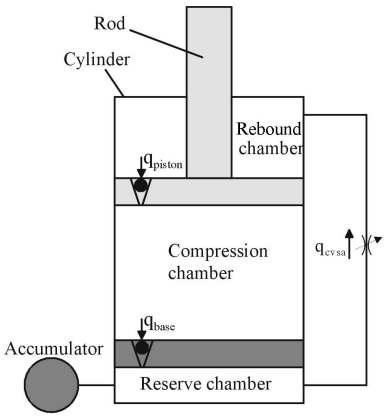

Figure 9: Semi-active damper.

control. In the figure, the vector $\mathbf{a}^c$ denotes the accelerations measured at the four corners of the car-body, $\mathbf{a}^m$, the modal accelerations, $\mathbf{g}^m$, the desired modal forces, $\mathbf{g}^d$, the desired damper forces, $d\mathbf{l}/dt$, the extension rates of the dampers, and $\mathbf{i}$, the electrical currents.

For the simulation of a normal manoeuver, a constant step-size $h = 0.01$ s has been selected, the implementation of a more sophisticated adaptive method being currently under development. The algorithmic parameters for the mechanical generalized coordinates are defined according to Eqn. (12) with $\rho_\infty = 0.9$, and the same parameters are used for the control sates. Since the control system is based on accelerometer measurements, it was very important to guarantee second-order accuracy at acceleration level. Our algorithm, which naturally fulfills this requirement, has a clear advantage over classical implementations based on a weighted residual formulation of the mechanical equations of motion.

In particular, a lane change maneuver has been simulated (Fig. 11). The car has a 10 m/s initial velocity, and a driver applies an open-loop steering command, without any real-time correction (blind driver assumption). The engine and the brakes do not produce any torque on the wheels. The simulation has been carried out within a reasonable computational time (a few minutes on a desk computer). Figure 12 illustrates the horizontal trajectory of the car. Due to the lateral sliding of the wheels and the open-loop nature of the driving command, a lateral drift is observed in the trajectory. Figure 13 presents the pitch and roll angles of the car-body. The dynamic behavior of the semi-active shock absorbers is analyzed in Fig. 14 and 15. Saturation phenomena dominate the variations of the electrical currents. The pressure in the compression

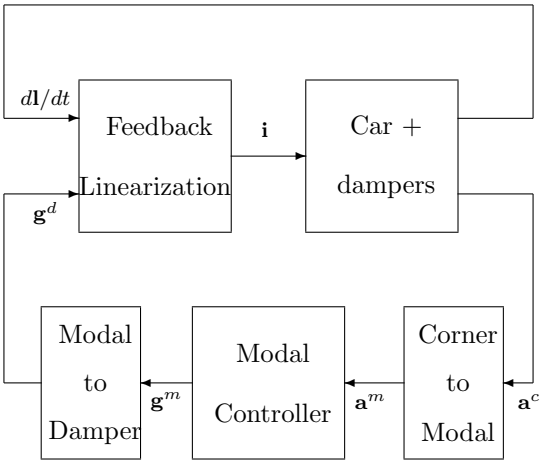

Figure 10: Semi-active control strategy.

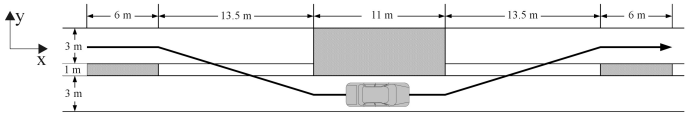

Figure 11: Lane change manoeuver (standard qualification test).

chamber is very low during the extending phase, but it is close to the pressure in the rebound chamber during the compression phase. All those results are physically consistent, and can be of great use in a pre-prototyping design phase or to improve the control algorithm.

CONCLUSIONS

This paper describes a consistent formulation of the generalized-α method for mechanical and mechatronic systems. The algorithm can deal with a non-constant mass matrix, controller dynamics, and kinematic constraints without resorting to any constraint regularization (i.e. constraints are only imposed at position level). Different integration formulae can be used for the mechanical generalized coordinates and for the control state variables. In contrast to other approaches, the recurrence relation for acceleration-like variables is formulated at acceleration level and not at force level, resulting in second-order accuracy for the acceleration variables. This property is especially useful for the simulation of mechatronic systems with acceleration feedback.

The theoretical background relies on the analogy with multistep formulae. For variable step-size schemes, we have shown that the classical order condition should be restated as an update condition for the numerical parameters γ and θ, which are thus modified at each time step. For constant step-size algorithms, a global convergence analysis has been realized, and we have proven that the method is convergent of order two when applied to mechatronic systems without kinematic constraints. In particular, different parameters can be selected for the mechanical generalized coordinates and for the control states without any degradation of the order of accuracy. Similar convergence results are also reported for constrained systems.

The theoretical results have been verified for a controlled spring-mass system. Moreover,

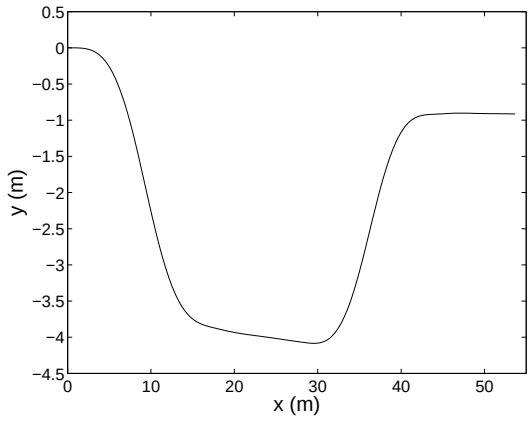

Figure 12: Horizontal trajectory of the car-body.

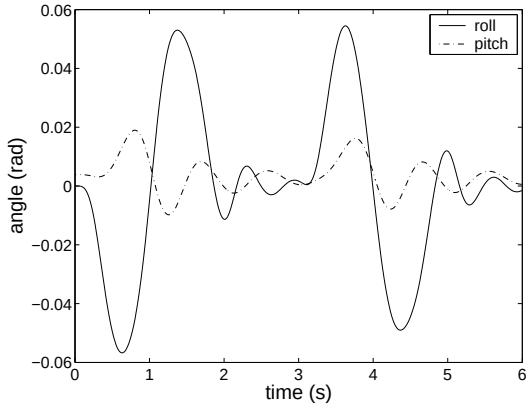

Figure 13: Angles of the car-body.

the algorithm has been applied with success to the simulation of a vehicle semi-active suspension. The numerical results demonstrate the ability of the proposed method to deal with industrial mechatronic systems.

Acknowledgments

O. Brüls is supported by a grant from the Belgian National Fund for Scientific Research (FNRS) which is gratefully acknowledged. This work also presents research results of the Belgian Program on Inter-University Poles of Attraction initiated by the Belgian state, Prime Minister's office, Science Policy Programming. The scientific responsibility rests with its authors.

References

[1] Chung, J., and Hulbert, G., 1993. "A time integration algorithm for structural dynamics with improved numerical dissipation: The generalized-α method". *ASME Journal of Applied Mechanics,* **60**, pp. 371–375.

[2] Erlicher, S., Bonaventura, L., and Bursi, O., 2002. "The analysis of the generalized-α method for non-linear dynamic problems". *Computational Mechanics,* **28**, pp. 83–104.

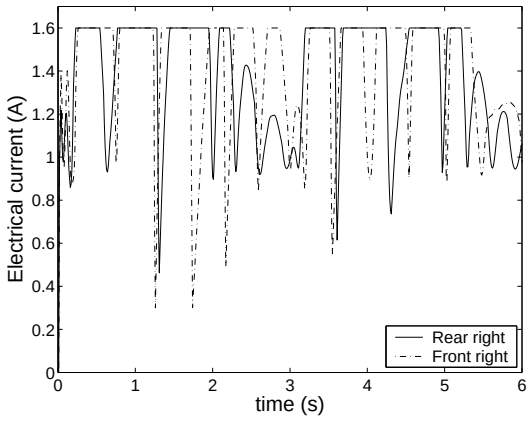

Figure 14: Electrical current in the valves.

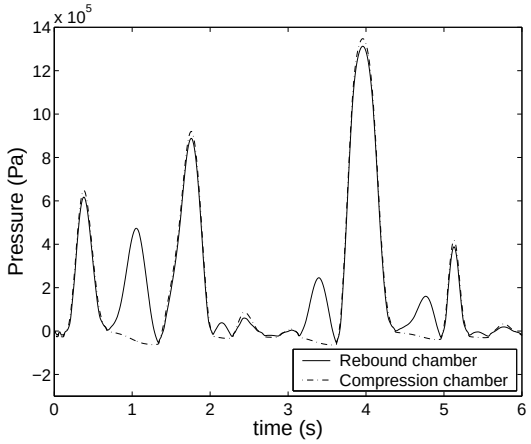

Figure 15: Hydraulic pressures in the rear right damper.

[3] Brüls, O., 2005. "Integrated simulation and reduced-order modeling of controlled flexible multibody systems". PhD thesis, University of Liège, Belgium.

[4] Brüls, O., and Golinval, J.-C., 2006. "The generalized-α method in mechatronic applications". *Zeitschrift für Angewandte Mathematik und Mechanik (ZAMM),* **86**(10), pp. 748–758.

[5] Brüls, O., and Golinval, J.-C., 2008. "On the numerical damping of time integrators for coupled mechatronic systems". *Computer Methods in Applied Mechanics and Engineering,* **197**(6–8), pp. 577–588.

[6] Cardona, A., and Géradin, M., 1989. "Time integration of the equations of motion in mechanism analysis". *Computers and Structures,* **33**, pp. 801–820.

[7] Lunk, C., and Simeon, B., 2006. "Solving constrained mechanical systems by the family of Newmark and α-methods". *Zeitschrift für Angewandte Mathematik und Mechanik (ZAMM),* **86**(10), pp. 772–784.

[8] Jay, L., and Negrut, D., 2007. "Extensions of the HHT-method to differential-algebraic equations in mechanics". *Electronic Transactions on Numerical Analysis,* **26**, pp. 190–208.

[9] Arnold, M., and Brüls, O., 2007. "Convergence of the generalized-α scheme for constrained mechanical systems". *Multibody System Dynamics,* **18**(2), pp. 185–202.

[10] Géradin, M., and Cardona, A., 2001. *Flexible Multibody Dynamics: A Finite Element Approach.* John Wiley & Sons, New York.

[11] Brenan, K., Campbell, S., and Petzold, L., 1996. *Numerical Solution of Initial–Value Problems in Differential–Algebraic Equations*, 2nd ed. SIAM, Philadelphia.

[12] Jansen, K., Whiting, C., and Hulbert, G., 2000. "A generalized-α method for integrating the filtered Navier-Stokes equations with a stabilized finite element method". *Computer Methods in Applied Mechanics and Engineering,* **190**, pp. 305–319.

[13] Hairer, E., Norsett, S., and Wanner, G., 1993. *Solving Ordinary Differential Equations I - Nonstiff Problems*, 2nd ed. Springer-Verlag.

[14] Hairer, E., and Wanner, G., 1996. *Solving Ordinary Differential Equations II - Stiff and Differential-Algebraic Problems*, 2nd ed. Springer-Verlag.

[15] Lauwerys, C., Swevers, J., and Sas, P., 2004. "Model free design for a semi-active suspension of a passenger car". In Proc. of ISMA 2004.